PAGEOPH, Vol. 139, No. 3/4 (1992) 0033-4553/92/040781-20$1.50 + 0.20/0
© 1992 Birkhäuser Verlag, Basel

Moment Tensors of Ten Witwatersrand Mine Tremors

A. McGARR[1]

Abstract—Ground motions, recorded both underground and on the surface in two of the South African Gold mining districts, were inverted to determine complete moment tensors for 10 mining-induced tremors in the magnitude range 1.9 to 3.3. The resulting moment tensors fall into two separate categories. Seven of the events involve substantial coseismic volumetric reduction $-\Delta V$ together with normal faulting entailing shear deformation $\sum AD$, where the summation is over fault planes of area A and average slip D. For these events the ratio $-\Delta V/\sum AD$ ranges from 0.58 to 0.92, with an average value of 0.71. For the remaining three events ΔV is not significantly different from zero; these events are largely double-couple sources involving normal faulting. Surprisingly, the two types of source mechanism appear to be very distinct in that there is not a continuous distribution of the source mix from $\Delta V = 0$ to $-\Delta V \sim \sum AD$. Presumably, the coseismic closure indicates substantial interaction between a mine stope and adjacent shear failure in the surrounding rock, under the influence of an ambient stress for which the maximum principal stress is oriented vertically.

Key words: Induced seismicity, earthquake source mechanism, implosive moment tensor component.

Introduction

Although the nature of source mechanisms of mining-induced tremors has been a controversial topic (e.g., WONG and McGARR, 1990), recent studies have provided definitive demonstrations of nonshear components in the moment tensors of some of these events. FEIGNIER and YOUNG (1992) inverted accelerometer recordings of microseismic events in the Underground Research Laboratory, Manitoba, to determine moment tensors and found events with both explosive and implosive components. STICKNEY and SPRENKE (1992) used a very comprehensive seismograph network to demonstrate that the P wave initial motions for tremors in the Coeur d'Alene mining district, Idaho, required a significant implosive component to the source mechanism.

The point of departure for this study is a brief report by McGARR (1992) describing the results of an analysis of ground motion for a mine tremor in South Africa recorded at small hypocentral distance both at an underground site and on the surface. The displacement waveforms, derived from accelerograms, were

[1] U.S. Geological Survey, MS 977, Menlo Park, CA 94025, U.S.A.

processed using a linear least-squares inversion technique to determine the complete moment tensor, which showed a substantial component of volume reduction; specifically I found that $-\Delta V/AD = 0.75$, where $-\Delta V$ is the volume decrease and AD is the product of fault area and average slip. In addition to describing the moment tensor inversion technique in more detail than before, this study expands the scope of the analysis from a single event to ten tremors recorded in two gold mining districts of the Witwatersrand.

For three yrears, from early 1986 to early 1989, the U.S. Geological Survey operated a seven-station seismic network (Figure 1) in and around the Witwatersrand gold fields (McGarr *et al.*, 1989). In addition to three continuously recording stations situated several hundred kilometers outside the gold fields, four GEOS digital event recorders (Borcherdt *et al.*, 1985) were installed at the surface of each of the four most seismically active mining districts. During three short-term experiments, each of several weeks duration, GEOS recorders were installed at underground sites within the two districts having the highest levels of seismicity. In November, 1986, two recorders were installed in the Western Deep Levels gold mine in the Carletonville district at depths of about 3000 and 1800 m. During two experiments in early 1988 and 1989, one GEOS unit was installed at a depth of 2065 m in the Vaal Reefs mine to record data in conjunction with the nearby surface recorder HBF. Both velocity and acceleration were recorded at sampling rates of either 200 or 400 per second. The ten tremors, which are the subject of this report, were recorded during these three special experiments.

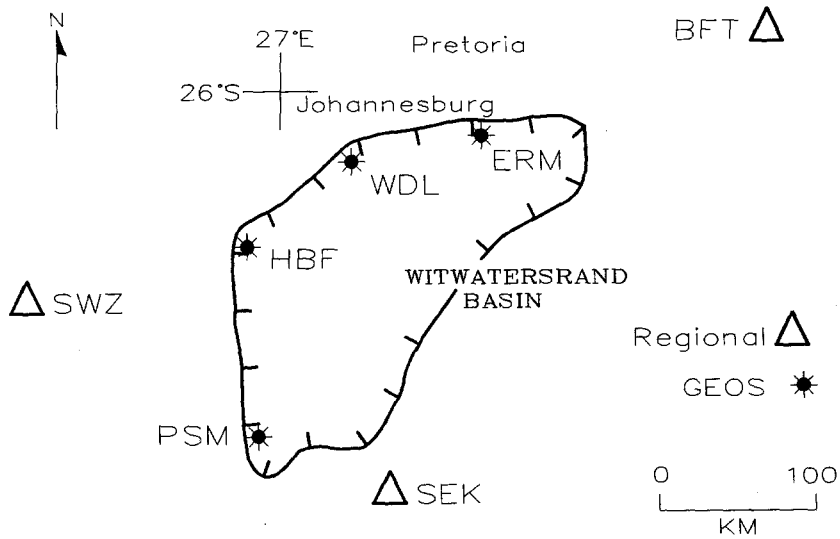

Figure 1
USGS seismic network in and around major gold mining districts of South Africa, ERM, WDL, HBF, and PSM denote GEOS stations and SWZ, SEK, and BFT are the regional stations. The special experiments of underground recording with GEOS units took place under WDL and HBF.

Mining-induced tremors in each of the two regions considered here are routinely located using extensive seismic networks involving geophones distributed throughout the mines; hypocentral location uncertainty typically ranges from 30 to 50 m. The vast majority of tremors, including all 10 of the report, are located within 150 m of a mine stope (e.g., COOK, 1963; MCGARR *et al.*, 1975).

The principal objective of this study was to assess the diversity in the moment tensors, including in particular, the mix of shear deformation and coseismic volume change. Earlier studies based on *P* wave initial motions had suggested sources with some coseismic volumetric reduction (e.g., JOUGHIN, 1966; VAN DER HEEVER, 1982) as well as double-couple sources (POTGIETER and ROERING, 1984).

Motivation

The moment tensor analysis in this report arose from frustation I was experiencing in trying to fit a double-couple mechanism to the ground displacement data shown in Figure 2. This tremor, event 0301411 (the first three digits, in this

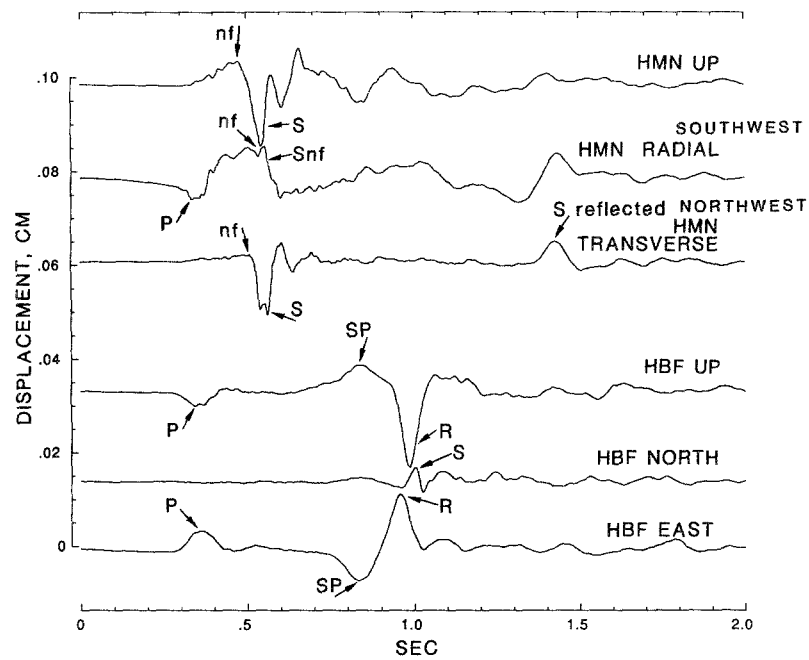

Figure 2

Event 030144 (Table 1) recorded at the underground site HMN and surface station HBF (Figure 3a). Ground acceleration recorded at 400 samples per second has been integrated twice to obtain displacement. Arrows indicate where the displacement was measured for purposes of determining the moment tensor. Note that the onset of *SV* (top trace) precedes significantly that of *SH* (third trace down); this may indicate wave velocity anisotropy.

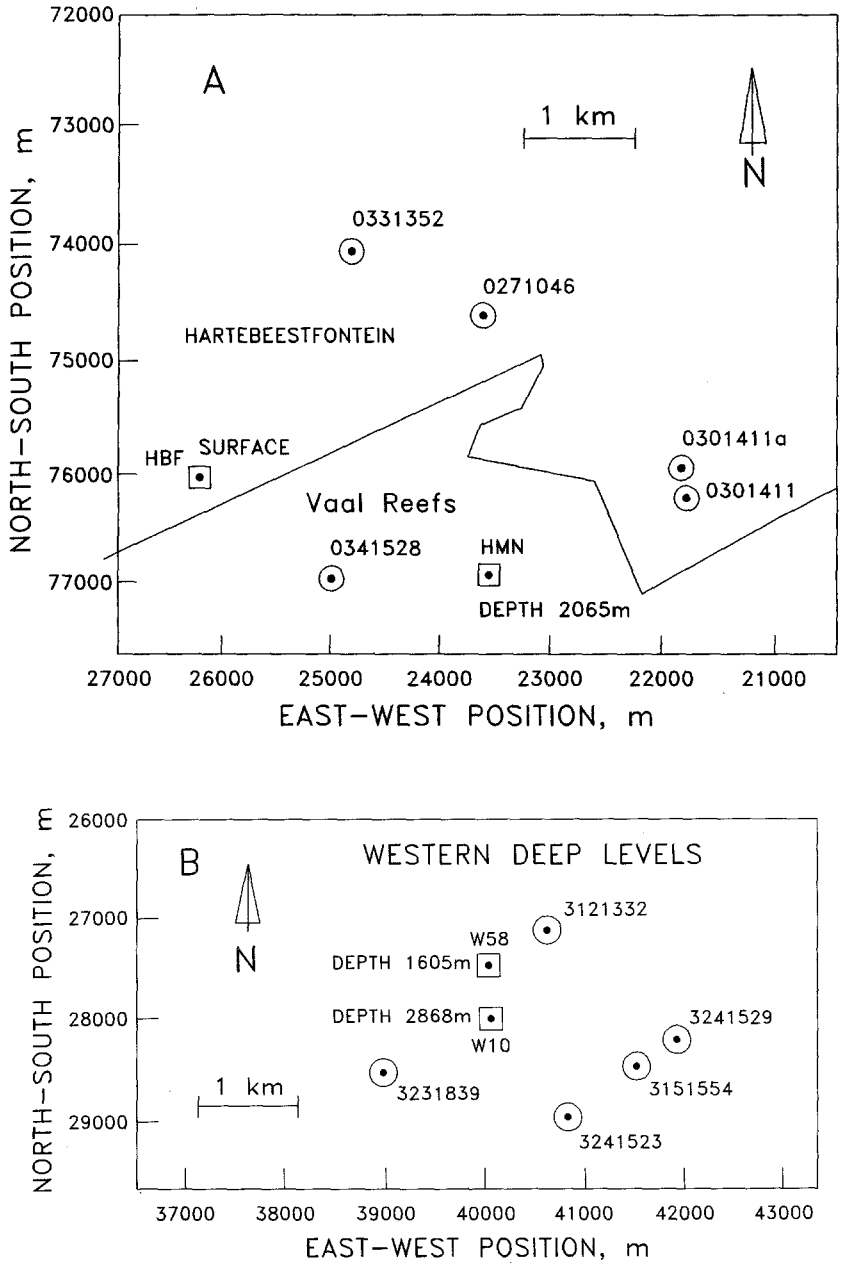

Figure 3

a. Map showing locations of events relative to GEOS stations HMN and HBF. The solid line dividing the map is the boundary between the Hartebeestfontein and Vaal Reefs gold mines. b. Map showing events in the Western Deep Levels Mine relative to recording stations W58 and W10.

nomenclature, indicate the Julian day and the last four the universal time) was recorded during the 1988 experiment and was located using the Klerksdorp district network (VAN DER HEEVER, 1984) in the Hartebeestfontein Mine, at a depth of 2125 m and 4.3 km east of the surface station HBF (Figure 3). The underground station, HMN, is located at similar depth as the event, and 1887 m to the southwest.

My intention was to use the surface data (HBF; bottom three traces of Figure 2) to determine the optimum double-couple source mechanism, employing the trial and error technique described by MCGARR and BICKNELL (1990). I would then calculate synthetic seismograms using this solution for the underground station HMN to confirm the validity of this double-couple mechanism, which involved slip across a normal fault striking approximately northward. To my consternation, this mechanism yielded waveforms for station HMN that were thoroughly out of accord with those observed (Figure 2). No amount of additional trial and error would rectify this problem. Contrary to my initial assumption that the data could be fit with a double-couple source (pp. 161–162 of GAY and WAINWRIGHT, 1984), it seemed that no such source would do; a volumetric component to the mechanism was apparently needed.

To understand why the ground motion of Figure 2 implies a substantial nonshear component in the source mechanism, consider equations (4.32) and (4.33) of AKI and RICHARDS (1980). Reprinted here, the solution for a point double-couple source is

$$\begin{aligned}\mathbf{u}(\mathbf{x}, t) = &\frac{1}{4\pi\rho}\mathbf{A}^N\frac{1}{r^4}\int_{r/\alpha}^{r/\beta}\tau M_0(t-\tau)\,d\tau \\ &+\frac{1}{4\pi\rho\alpha^2}\mathbf{A}^{IP}\frac{1}{r^2}M_0\left(t-\frac{r}{\alpha}\right)+\frac{1}{4\pi\rho\beta^2}\mathbf{A}^{IS}\frac{1}{r^2}M_0\left(t-\frac{r}{\beta}\right) \\ &+\frac{1}{4\pi\rho\alpha^3}\mathbf{A}^{FP}\frac{1}{r}\dot{M}_0\left(t-\frac{r}{\alpha}\right)+\frac{1}{4\pi\rho\beta^3}\mathbf{A}^{FS}\frac{1}{r}\dot{M}_0\left(t-\frac{r}{\beta}\right),\end{aligned} \tag{1a}$$

where

$$\begin{aligned}\mathbf{A}^N &= 9\sin 2\theta\cos\phi\hat{\mathbf{r}} - 6(\cos 2\theta\cos\phi\hat{\boldsymbol{\theta}} - \cos\theta\sin\phi\hat{\boldsymbol{\phi}}) \\ \mathbf{A}^{IP} &= 4\sin 2\theta\cos\phi\hat{\mathbf{r}} - 2(\cos 2\theta\cos\phi\hat{\boldsymbol{\theta}} - \cos\theta\sin\phi\hat{\boldsymbol{\phi}}) \\ \mathbf{A}^{IS} &= -3\sin 2\theta\cos\phi\hat{\mathbf{r}} + 3(\cos 2\theta\cos\phi\hat{\boldsymbol{\theta}} - \cos\theta\sin\phi\hat{\boldsymbol{\phi}}) \\ \mathbf{A}^{FP} &= \sin 2\theta\cos\phi\hat{\mathbf{r}} \\ \mathbf{A}^{FS} &= \cos 2\theta\cos\phi\hat{\boldsymbol{\theta}} - \cos\theta\sin\phi\hat{\boldsymbol{\phi}}.\end{aligned} \tag{1b}$$

Ground displacement $\mathbf{u}$, in a whole space, is a function of density ρ, hypocentral distance r, compressional and shear wave velocities α and β, and the time dependent seismic moment $M_0(t)$; $M_0(t) = 0$ for $t \leq 0$ and $M_0(\infty) = \mu AD$, where μ is the modulus of rigidity. Additionally, $M_0(t)$ is assumed to be a monotonic function.

The radiation factors of (1b) involve a polar coordinate system for which the angle θ is measured from the normal to the fault and ϕ is the angle within the fault plane measured from the slip vector; $\hat{\mathbf{r}}$, $\hat{\boldsymbol{\theta}}$, and $\hat{\boldsymbol{\phi}}$ are unit vectors in the coordinate directions. The terms in (1a) involving $\mathbf{A}^{IP}$ and $\mathbf{A}^{FP}$ begin at time r/α, those with $\mathbf{A}^{IS}$ and $\mathbf{A}^{FS}$ at r/β, and that with $\mathbf{A}^{N}$ increases in amplitude between the P- and S-wave arrival times r/α and r/β.

The terms in (1a) involving $\mathbf{A}^{N}$, $\mathbf{A}^{IP}$ and $\mathbf{A}^{IS}$ comprise the near-field radiation because of their dependence on hypocentral distances as $1/r^2$, in contrast to that of the far-field body waves ($\mathbf{A}^{FP}$, $\mathbf{A}^{FS}$) for which the distance dependence is $1/r$. For the term with $\mathbf{A}^{N}$ the $1/r^2$ distance dependence only becomes apparent after integration.

The most clear-cut problem with fitting a double-couple source model to event 0301411 is an essential incompatibility between the southwest (radial) component of ground motion at HMN (Figure 2) and the corresponding solution of (1) for which only those terms involving $\hat{\mathbf{r}}$ (1b) can contribute. Whereas one observes a northeastward P pulse followed by southwestward increasing ground motion between the P and S arrivals (Figure 2) the solution in (1) indicates that these two phases must have the same radial polarity; that is, the $\hat{\mathbf{r}}$ components of $\mathbf{A}^{N}$, $\mathbf{A}^{IP}$ and $\mathbf{A}^{FP}$ all have the same sign. Moreover, the near-field S wave is observed to be a northeastward step on the radial component, and thus, has the same radial polarity as the P wave. In contrast, equations (1) indicate the opposite polarity for these phases (the terms involving $\mathbf{A}^{FP}$ and $\mathbf{A}^{IS}$). Hence, the double-couple source, normally assumed for earthquakes, cannot satisfy the ground motion for event 0301411 as recorded at HMN (Figure 2).

Moment Tensor Inversion

Having ruled out a double-couple source mechanism for event 0301411, I concluded that it would be most realistic to assume a general moment tensor source. As outlined in McGarr (1992), to determine the required tensor one can invert linearly (Stump and Johnson, 1977; Gibowicz, 1990)

$$A_{ij}m_j = u_i \tag{2}$$

which relates the moment tensor m_j, expressed as a vector (M_{xx}, M_{yy}, M_{zz}, M_{xy}, M_{xz}, M_{yz}) to the observed ground motion u_i. The x, y and z axes are oriented along the east, north and up directions.

The u_i consists of the 15 measurements of ground motion made at the points indicated in Figure 2. One unusual arrival at HMN that helped to provide source definition is the transverse shear wave reflected from the surface.

To determine the matrix A_{ij}, synthetic seismograms were calculated for each component m_j for comparison with the observations (Figure 2). All components of

the moment tensor are assumed to have the same time history taken here as (McGARR, 1991)

$$\begin{aligned} \dot{M}_0(t)/M_0 &= f(1-\cos 2\pi ft) \quad \text{for } 0 \le t \le 1/f \\ &= 0 \qquad\qquad\qquad\quad \text{otherwise} \end{aligned} \tag{3}$$

f, the inverse period of the far-field displacement pulse, is determined from the S waves recorded underground; for event 0301411 the vertical component at HMN indicated that $f = 6$ Hz. To calculate seismograms for paths to the underground site HMN, equation (4.29) of AKI and RICHARDS (1980) was evaluated. For the surface site HBF I used a program provided by L. R. Johnson (written communication, 1977) that is based on a technique described by JOHNSON (1974). For paths to the underground stations α and β are taken as 6 and 3.6 km/s. For paths to surface station HBF β is reduced to 3.4 km/s.

Thus, the components of the A_{ij} matrix are the measurements from the synthetic seismograms, for each m_j, corresponding to the actual ground motion measurements (Figure 2). As seen in Figure 4, 15 measurements each were made for sets of seismograms for the M_{xx} and M_{zz} components. Note that, whereas M_{xx} yields a substantial P wave on the radial component of HMN, M_{zz} produces no P wave, but

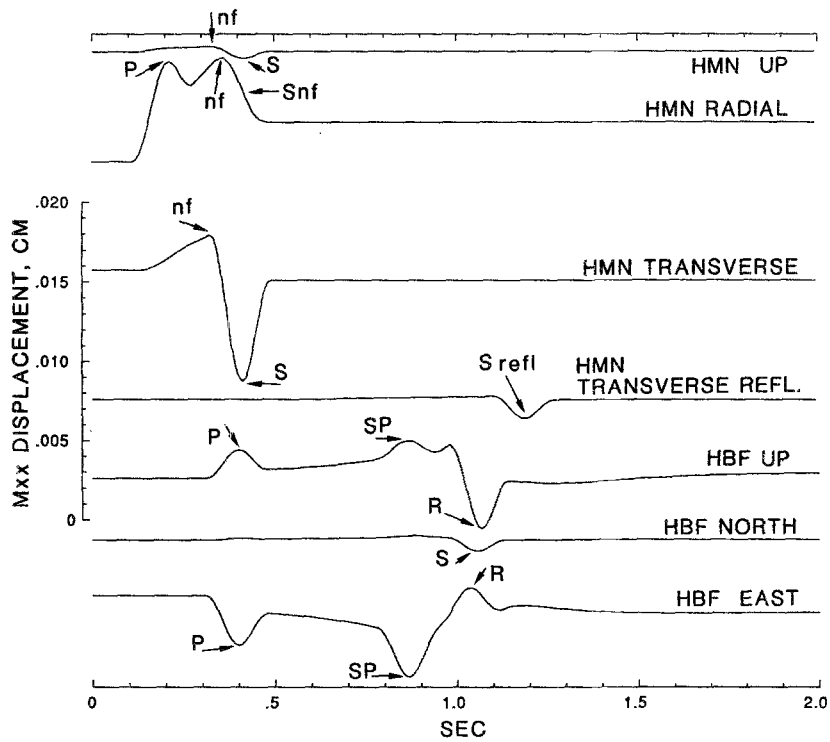

Figure 4(a)

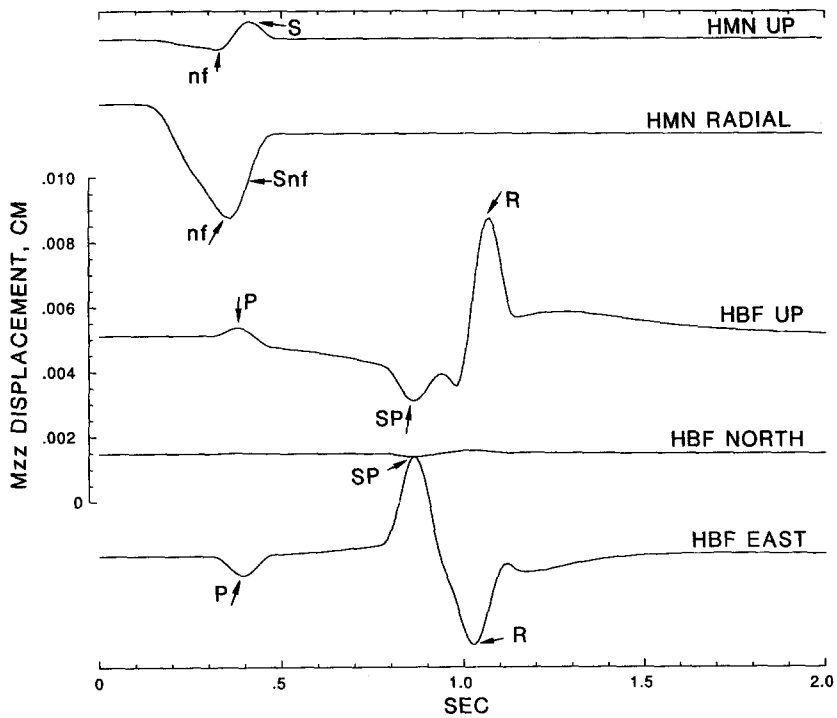

Figure 4(b)

Figure 4

a. Synthetic seismograms of M_{xx} component for ray paths for event 0301411 to HMN and HBF. The phases reflected from the free surface, calculated separately, are computed as though the station HMN is situated at its image point above the surface. b. Same as Figure 4a but for M_{zz}, which produces no transverse ground motion.

a relatively large near-field ramp that increases in amplitude between the P and S wave arrival times.

Once the A_{ij} matrix is determined (90 measurements in the case of event 0301411) then the linear equations (2) are solved using a standard least-squares technique. The results for event 0301411 is

$$M_{ij} = \begin{bmatrix} -0.22 \pm 0.07 & -0.06 \pm 0.07 & 0.14 \pm 0.06 \\ & -0.54 \pm 0.21 & -0.06 \pm 0.11 \\ & & -1.00 \pm 0.23 \end{bmatrix} \times 1.82 \times 10^{14} \text{ N-m.} \quad (4)$$

Only the independent components of the moment tensor are shown as well as the one sigma uncertainties. To demonstrate the validity of this solution, synthetic seismograms, with $f = 6$ Hz, are compared to the observations in Figure 5, where we see that that the calculated and observed waveforms agree quite well for both HMN and HBF.

In the moment tensor of (4), the diagonal elements predominate and are all negative thus indicating that the source involves a substantial component of

coseismic volume reduction. From the trace of (4), this coseismic volume change ΔV can be calculated from

$$\Delta V = \mathrm{tr}(M_{ij})/(3\lambda + 2\mu) \tag{5}$$

where λ and μ are Lamé's elastic moduli. For the quartzitic strata in the environs of the tremors, $3\lambda + 2\mu = 1.63 \times 10^5$ MPa. From (4), $\mathrm{tr}(M_{ij}) = 3.20 \times 10^{14}$ N-m and then from (5), $\Delta V = -1980\ \mathrm{m}^3$.

To estimate the deviatoric component of the moment tensor for comparison with the isotropic (volume change) component, M_{ij} is first diagonalized and then decomposed into volumetric and deviatoric components according to

$$M(\mathrm{dev}) = M(\mathrm{diag}) - \tfrac{1}{3}\begin{bmatrix} \mathrm{tr}(M_{ij}) & & \\ & \mathrm{tr}(M_{ij}) & \\ & & \mathrm{tr}(M_{ij}) \end{bmatrix}. \tag{6}$$

For event 0301411

$$M(\mathrm{diag}) = \begin{bmatrix} -0.18 & & \\ & -0.52 & \\ & & -1.00 \end{bmatrix} \times 1.89 \times 10^{14}\ \text{N-m} \tag{7}$$

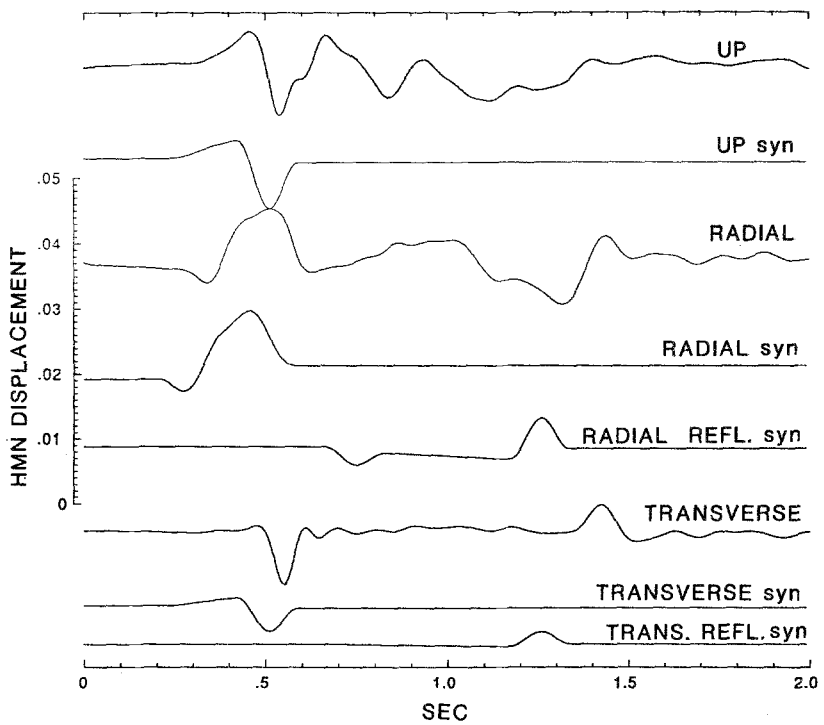

Figure 5(a)

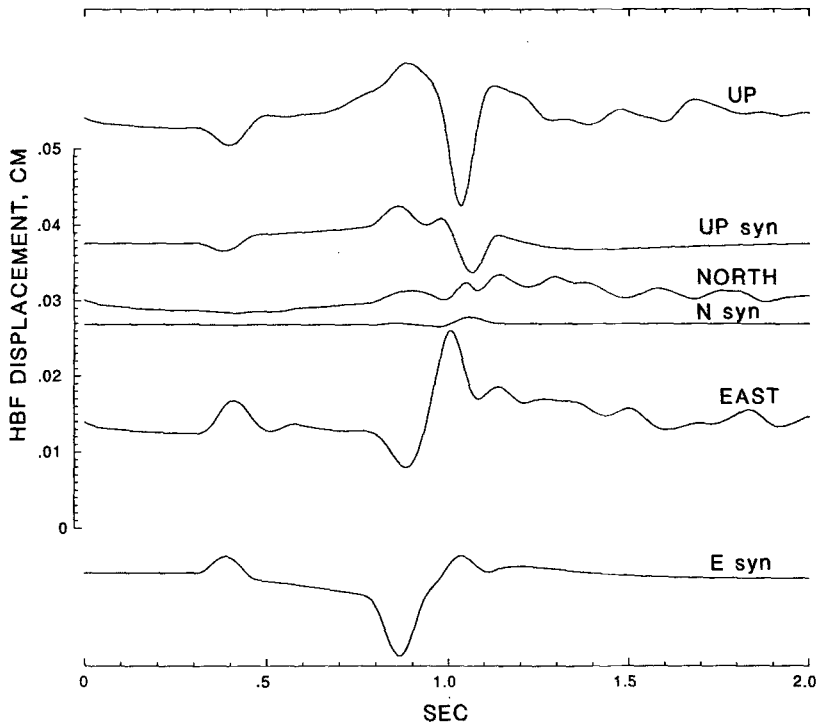

Figure 5(b)

Figure 5

a. Observed and synthetic seismograms for event 0301411 at station HMN. Synthetic traces are calculated on the basis of (4) with $f = 6$ Hz in (3). The surface reflections, calculated separately, are for HMN at its image point above the surface and assuming that $\beta = 3.4$ km/s instead of 3.6 km/s used for direct paths to HMN. b. Observed and synthetic seismograms, calculated from (4), for surface station HBF.

with eigenvectors $(0.98, 0.14, 0.16)$, $(0.16, -0.99, -0.13)$, and $(-0.14, -0.15, -0.99)$. Hence, the principal moments are aligned essentially along east, north, and up in order of increasing magnitude. Then, applying (6) to (7) yields

$$M(\text{dev}) = \begin{bmatrix} 0.39 & & \\ & 0.04 & \\ & & -0.43 \end{bmatrix} \times 1.89 \times 10^{14} \text{ N-m} \tag{8}$$

with the same eigenvectors as for (7).

This deviatoric moment tensor can be expressed as a sum of double-couple tensors, but not uniquely (e.g., JOST and HERRMANN, 1989). The decomposition used here is straightforward in that it preserves the principal moment directions.

The deviatoric moment tensor can be written in general as

$$M(\text{dev}) = \begin{bmatrix} M_1(\text{dev}) & & \\ & M_1(\text{dev}) & \\ & & -[M_1(\text{dev}) + M_2(\text{dev})] \end{bmatrix} \tag{9}$$

where $M_1(\text{dev})$ and $M_2(\text{dev})$ are assumed to have the same sign. Then, in terms of double-couples,

$$M(\text{dev}) = \begin{bmatrix} M_1(\text{dev}) & & \\ & 0 & \\ & & -M_1(\text{dev}) \end{bmatrix} + \begin{bmatrix} 0 & & \\ & M_2(\text{dev}) & \\ & & -M_2(\text{dev}) \end{bmatrix}. \tag{10}$$

In the case of event 0301411, applying (10) to (8) gives

$$M(\text{dev}) = \left\{ \begin{bmatrix} 0.39 & & \\ & 0 & \\ & & -0.39 \end{bmatrix} + \begin{bmatrix} 0 & & \\ & 0.04 & \\ & & -0.04 \end{bmatrix} \right\} \times 1.89 \times 10^{14} \text{ N-m.} \tag{11}$$

Thus, the deviatoric component of the moment tensor of event 0301411 is largely a double-couple source with P and T axes oriented close to vertical and east, respectively. The much smaller component has the same P axis and a T axis oriented northerly.

Each of the double-couple terms in (10) has scalar seismic moment $\mu AD = M_i(\text{dev})$, where i is 1 or 2. Accordingly, scalar addition of the two components in (10) yields a measure of the total shear deformation

$$M_0 = \mu \sum AD = M_1(\text{dev}) + M_2(\text{dev}). \tag{12}$$

For event 0301411 with modulus of rigidity $\mu = 3.76 \times 10^4$ MPa, (12) yields $\sum AD = 2160 \text{ m}^3$, which is somewhat greater than the volumetric reduction of 1980 m^3, found before, for this same event.

To recapitulate, using event 0301411 as an example, I have indicated the procedure by which measurements of ground displacement, recorded locally are inverted to determine the moment tensor best representing the source. From the resulting moment tensor, both the coseismic volume change and the shear deformation can be determined, as well as the scalar seismic moment M_0, which is a measure of the total shear deformation; M_0, in turn, yields a moment-magnitude (HANKS and KANAMORI, 1979)

$$M = (\log M_0 - 16)/1.5. \tag{13}$$

Both events 0301411, used as an example while presenting the analysis techniques used here, and 0341528, analyzed in MCGARR (1992) have mechanisms involving coseismic volumetric reduction comparable in magnitude to the corresponding shear deformation; in both cases, ΔV is smaller in magnitude than $\sum AD$, but not by much. To get some idea of the diversity of the moment tensors for Witwater-

Table 1

Moment tensors and related data

Event	Year	Mine[a]	Depth m	M_{xx}	M_{yy}	M_{zz}	M_{xy}	M_{xz}	M_{yz}	tr(M_{ij})	Scale Factor[b] N-m	f Hz
3121332	1986	WDL	2683	-0.26 ± 0.14	-0.25 ± 0.11	-1.00 ± 0.10	-0.11 ± 0.06	0.10 ± 0.05	0.19 ± 0.03	-1.51	1.12×10^{12}	30
3231839	1986	WDL	2822	0.20 ± 0.14	1.00 ± 0.28	-0.78 ± 0.14	0.28 ± 0.13	-0.39 ± 0.10	-0.24 ± 0.13	0.42	3.9×10^{12}	18
3241523	1986	WDL	3243	-0.08 ± 0.10	-0.64 ± 0.08	-1.00 ± 0.09	-0.06 ± 0.05	0.24 ± 0.05	0.28 ± 0.05	-1.72	2.8×10^{12}	25
3241529	1986	WDL	3100	0.16 ± 0.19	0.35 ± 0.30	0.01 ± 0.29	0.35 ± 0.10	-1.00 ± 0.17	-0.06 ± 0.18	0.52	3.75×10^{12}	25
3151554	1986	WDL	2205	-0.24 ± 0.13	-0.40 ± 0.26	-1.00 ± 0.18	0.16 ± 0.11	-0.31 ± 0.09	0.23 ± 0.12	-1.64	7.40×10^{12}	13
0301411	1988	HBF	2125	-0.22 ± 0.07	-0.54 ± 0.21	-1.00 ± 0.23	0.06 ± 0.07	0.14 ± 0.06	-0.06 ± 0.11	-1.76	1.82×10^{14}	6
0301411a[c]	1988	HBF	2055	-0.11 ± 0.06	-0.68 ± 0.19	-1.00 ± 0.16	-0.02 ± 0.07	-0.09 ± 0.08	0.44 ± 0.17	-1.79	3.87×10^{13}	8
0331352	1988	HBF	2145	0.89 ± 1.07	-0.51 ± 0.30	-0.30 ± 0.33	0.02 ± 0.51	-0.46 ± 0.67	-1.00 ± 0.48	0.08	1.44×10^{12}	22
0341528	1988	VR	2060	-0.30 ± 0.06	-0.35 ± 0.17	-1.00 ± 0.10	-0.04 ± 0.02	0.21 ± 0.05	-0.02 ± 0.05	-1.65	8.68×10^{12}	13
0271046	1989	HBF	1918	-0.31 ± 0.23	-0.45 ± 0.15	-1.00 ± 0.18	-0.12 ± 0.06	-0.01 ± 0.17	-0.13 ± 0.10	-1.76	1.39 ± 10^{13}	13

[a] WDL: Western Deep Levels; HBF: Hartebeestfontein; VR: Vaal Reefs.

[b] Moment tensor components and tr(M_{ij}) should be multiplied by this factor.

[c] Event 0301411a occurred less than 1 minute after 0301411.

srand mine tremors, eight additional events with clearly recorded ground motion from the three special experiments were analyzed, using the methodology just described.

Five of the eight events (Table 1) were recorded during the first experiment involving underground recording at two depths in the Two Shaft area of the Western Deep Levels (WDL) mine (Figure 3b); these two recording sites, W58 and W10, have little horizontal separation but the vertical distance between them exceeds 1200 m. Mining at Western Deep Levels is on two stratigraphic horizons, the shallower Ventersdorp Contact Reef and the deeper Carbon Leader Reef. For WDL events, depths near 3000 m in this area (Figure 3b) indicate those induced by mining the Carbon Leader whereas depths near 2000 m suggest an association with Ventersdorp Contact mining; thus, only event 3151554 (Table 1) was induced by the shallower mining.

I should mention that most of the events at WDL (Table 1) were recorded at the surface station of the same name (Figure 1), in addition to the two underground stations W58 and W10. Because of pronounced site resonances in the frequency band of interest, however, ground motion from WDL was of almost no use in the determination of moment tensors; this is in contrast to the surface station HBF in the Klerksdorp district (Figure 1) that proved very effective for constraining moment tensors (e.g., Figure 2).

Of the other five events analyzed here (Table 1), four were recorded in early 1988 and the fifth in early 1989, in the vicinity of underground site HMN and surface station HBF (Figure 3a). Because much of the mining in that district involves a single gently dipping reef, most of the induced tremors are at depths close to that horizon, typically somewhat below 2000 m. Accordingly, ray paths to HMN, at a depth of 2065 m, are nearly horizontal. Event 0341528 provided exceptionally definitive ground motion data (McGarr, 1992) because it is situated, in plan, between stations HMN and HBF (Figure 3a) resulting in very small epicentral distances. The waveforms of event 0301411 (Figure 2) are more typical for this study inasmuch as the epicentral distance to HBF substantially exceeds the vertical distance, resulting in some waveform complexity (e.g., S to P conversions, Figure 2).

The moment tensors listed in Table 1 fall into two categories. Seven of the moment tensors have traces that are significantly negative. For each of these events, M_{zz} is the largest component. Of particular significance, the magnitude of $\mathrm{tr}(M_{ij})$ is many times greater than twice the one sigma uncertainty associated with M_{zz} (Table 1). Thus, the negative traces of these seven events are statistically very significant.

The other three events fall in the second category for which the moment tensor traces are positive, but not significantly so. For each of these events, $\mathrm{tr}(M_{ij})$ is less than the two sigma uncertainty of the largest diagonal component. For event 3231839, for instance, $\mathrm{tr}(M_{ij}) = 0.42$ (Table 1) whereas the two sigma uncertainty of the largest diagonal component M_{yy} is 0.56. Statistically, then, for these three

events, tr(M) is not significantly different from zero and so these mechanisms are interpreted here as purely deviatoric. Event 3231839 is notable both as an example of data obtained during the 1986 WDL experiment (Figure 3b) and because its results provide a distinct contrast to those of event 0301411 (Figures 2 and 5). In Figure 6 we see observed and calculated (from the results of Table 1) displacement for both W10 and W58. The radial trace at W10 is of particular interest because the ray path, being horizontal, should yield P-wave and near-field motion, but no far-field S wave. Whereas the corresponding trace for event 0301411 (Figure 2) showed a radially inward P wave followed by an outward near-field ramp and an inward near-field S wave, for event 3231839 we see (Figure 6) radially outward P, outward ramp and inward near-field S, a combination that is compatible with the expectations of (1), the double-couple solution. Thus, even before inverting the ground displacement, as measured at 20 points, the data suggest a source more deviatoric than for event 0301411. As already described, the resulting moment tensor confirms the largely deviatoric nature of the source mechanism (Table 1) and the good agreement between observed and synthetic seismograms (Figure 6) at W10 and W58 validates the solution.

One final point with regard to the solutions in Table 1 involves the necessity for complete six-component moment tensors. For the three events with small but positive traces, six components are clearly not necessary; as the trace does not differ

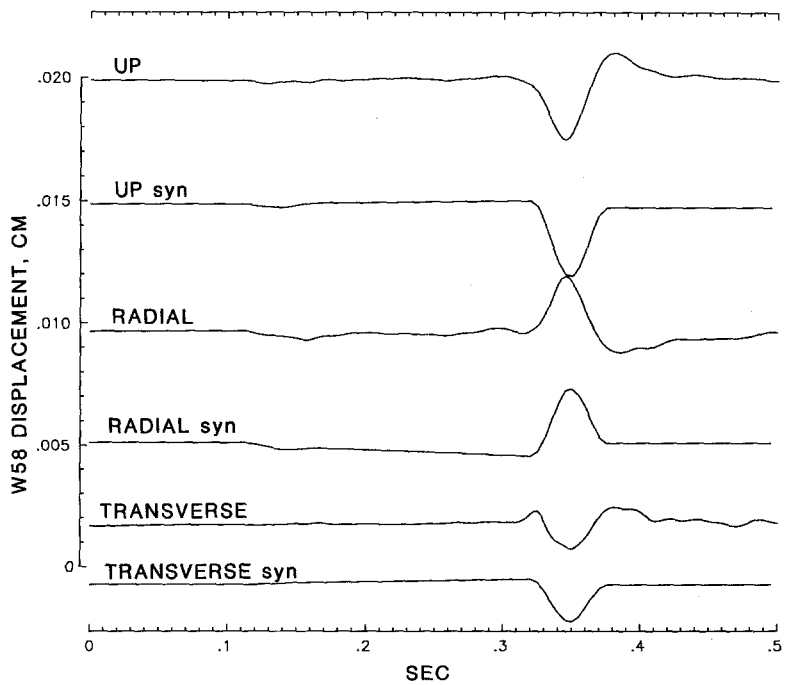

Figure 6(a)

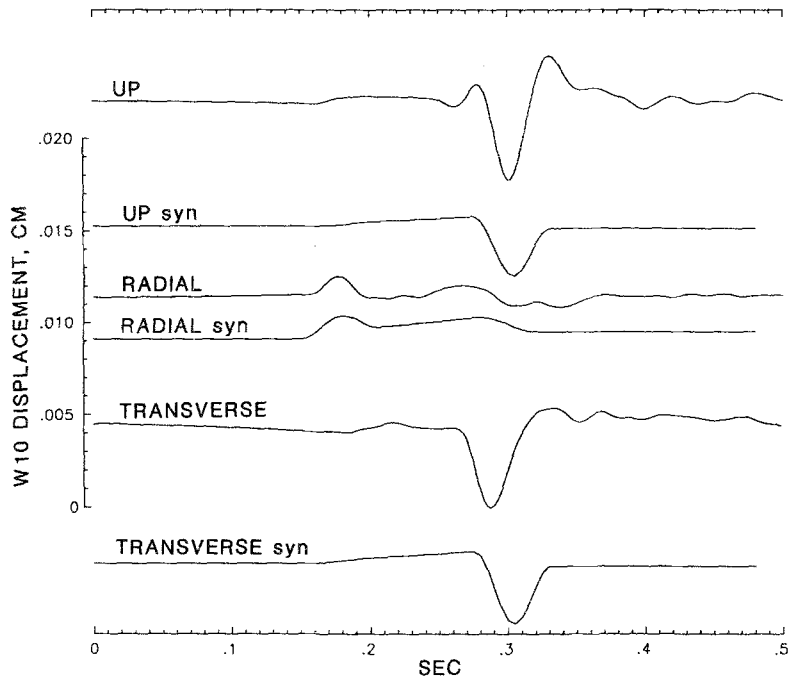

Figure 6(b)

Figure 6

a. Observed and calculated seismograms for event 3221839 at underground station W58 (Figure 3b). The observed displacement is derived from ground velocity recorded at 400 samples per second at both W58 and W10. The synthetic seismograms were calculated for the moment tensor solution given in Table 1.
b. Same as for 6a but for underground station W10.

significantly from zero, a moment tensor of five components with the trace constrained to zero, would certainly suffice. For the seven events with negative traces, however, the same test that was described in McGarr (1992) for event 0341528 (Table 1) indicates that moment tensors with zero trace and five independent components cannot satisfy the observations; the coseismic volume reduction is observationally required.

Source Mix

Table 2 summarizes the analysis of the moment tensor results for the ten events of this study. Consider the diagonalized moment tensors, represented as principal moments, M_i and corresponding eigenvectors, e_i. For each event, the principal moments are listed in order of increasing negative magnitude.

First, note that for most of the 10 events the orientation of M_3 is nearly vertical. Presumably, the alignment of M_3 indicates the way in which the near-vertical

Table 2

Diagonalized moment tensors and related results

Event	M_1	e_1^*	M_2	e_2^*	M_3	e_3^*	Scale Factor N-m	$-\Delta V_3$† m³	ΣAD** m³	$-\Delta V/AD$	M_0(scalar)‡ N-m	$M^{(a)}$
3121332	−0.13	(−0.61, 0.78, 0.10)	−0.30	(−0.77, −0.57, −0.26)	−1.00	(0.15, 0.24, −0.96)	1.18×10^{12}	10.3	16.6	0.62	6.14×10^{11}	1.9
3231839	1.00	(−0.35, −0.92, 0.20)	0.14	(−0.89, 0.39, 0.26)	−0.77	(0.31, 0.08, 0.95)	4.56×10^{12}	−10.4	107.9	−0.10	4.06×10^{12}	2.4
3241523	−0.01	(0.97, 0.01, 0.24)	−0.41	(−0.12, 0.90, 0.43)	−1.00	(0.22, 0.45, −0.87)	3.37×10^{12}	29.4	47.1	0.62	1.75×10^{12}	2.2
3241529	1.00	(0.71, 0.33, −0.63)	0.22	(−0.13, 0.94, 0.34)	−0.79	(−0.69, 0.16, −0.71)	4.50×10^{12}	−12.0	111.3	−0.11	4.18×10^{12}	2.4
3151554	−0.10	(−0.91, −0.37, 0.18)	−0.27	(0.27, 0.86, −0.42)	−1.00	(−0.34, 0.32, −0.88)	8.90×10^{12}	74.5	129.0	0.58	4.85×10^{12}	2.5
0301411	−0.18	(0.98, 0.14, 0.16)	−0.52	(−0.16, −0.99, −0.13)	−1.00	(−0.14, −0.15, 0.99)	1.89×10^{14}	1980.0	2160.0	0.92	8.1×10^{13}	3.3
0301411a	−0.07	(−0.97, 0.17, 0.18)	−0.30	(0.24, 0.81, 0.54)	−1.00	(0.06, −0.57, 0.82)	5.09×10^{13}	426.0	731.0	0.58	2.75×10^{13}	3.0
0331352	0.82	(0.81, 0.34, −0.48)	0.25	(0.58, −0.62, 0.54)	−1.00	(0.12, 0.72, 0.69)	2.06×10^{12}	−0.71	55.9	−0.01	2.10×10^{12}	2.2
0341528	−0.21	(0.90, −0.35, 0.25)	−0.35	(−0.34, −0.94, −0.07)	−1.00	(−0.26, 0.02, 0.97)	9.16×10^{12}	88.0	117.0	0.75	4.40×10^{12}	2.4
0271046	−0.24	(0.90, −0.43, 0.07)	−0.45	(−0.43, −0.87, 0.22)	−1.00	(0.05, 0.22, 0.97)	1.44×10^{13}	150.0	165.0	0.91	6.19×10^{12}	2.5

* The coordinate system used here is (east, north, up).

† Calculated from (5).

** Calculated from (12), with $\mu = 3.76 \times 10^4$ MPa.

‡ Calculated from (12).

(a) Moment magnitude calculated from (13).

maximum principal stress (e.g., GAY, 1975; GAY *et al.*, 1984) interacts with the subhorizontal mine stopes to induce tremors (e.g., MCGARR *et al.*, 1975).

To describe additional features in common it is necessary to consider the events in the two categories described before, the seven for which the trace is substantially negative and the three that are essentially deviatoric solutions with no significant trace. Turning first to the larger category, we see numerous features in common. First, in all cases near-vertically oriented M_3 has the largest magnitude by a substantial margin. Second, the coseismic volume reduction $-\Delta V$, from (5), is of the same order as the shear deformation measured by $\sum AD$, from (12). This ratio $-\Delta V/\sum AD$ ranges from 0.58 to 0.92 about its mean of 0.71. This ratio shows no scale, or magnitude, dependence. Third, all of the negative trace events have principal moments that are all negative; this implies P-wave first motions that are exclusively dilatational for these seven events.

Turning now to the three events with small, positive moment tensor traces (Table 1), there are several points of interest. First, such events occur in both widely separated mining areas, around WDL and HBF. Second, the ratio of volume change to shear deformation is small and, as suggested before, not significantly different from zero.

Considering all ten events it is of considerable interest that there seems to be a clear separation in mechanism between the tremors with substantially negative traces and those without a significant trace. To date, at least, the data (Table 2) do not suggest a continuum in mechanisms from purely deviatoric to implosive/deviatoric; the moment tensors fall clearly in one category or the other.

Generally, the deviatoric principal moments M_i^* (Table 3) indicate normal faulting in that the largest negative component M_3^* tends to be oriented vertically

Table 3

Deviatoric principal moment tensor components[a] and R values

Event	M_1^*	M_2^*	M_3^*	Scale Factor N-m	R[b]
3121332	0.67	0.33	−1.00	6.14×10^{11}	−60
3231839	0.99	0.01	−1.00	4.06×10^{12}	17
3241523	0.88	0.12	−1.00	1.75×10^{12}	−58
3241529	0.92	0.08	−1.00	4.18×10^{12}	19
3151554	0.66	0.34	−1.00	4.85×10^{12}	−56
0301411	0.91	0.09	−1.00	8.13×10^{13}	−66
0301411a	0.72	0.28	−1.00	2.75×10^{13}	−56
0331352	0.78	0.22	−1.00	2.10×10^{12}	3
0341528	0.64	0.35	−1.00	4.40×10^{12}	−62
0271046	0.74	0.26	−1.00	6.19×10^{12}	−66

[a] Calculated using (6). The eigenvectors are the same as in Table 2.
[b] Calculated from (14).

(Table 2). For each event, the value of M_2^* shows whether the shear deformation is on one or several planes, with $M_2^* = 0$ implying a double-couple or single fault plane and $|M_2^*| = \frac{1}{2}$ diagnostic of slip equally distributed between the two orthogonal fault planes, also termed a compensated linear-vector dipole or CLVD (KNOPOFF and RANDALL, 1970). Magnitudes of M_2^* between 0 and $\frac{1}{2}$ suggest a major and a minor fault plane; mechanisms of this sort are termed "triple doublets" (GELLER, 1976). Considering the uncertainties in the analysis (Table 1) it seems realistic to consider values of $|M_2^*| < 0.15$ as zero, in which case five of the events (Table 3) have deviatoric components involving double-couple failure with the other five in the triple doublet category; there appear to be no CLVD mechanisms.

Another measure of the nature of the moment tensor was introduced by FEIGNIER and YOUNG (1992), who analyzed 33 microtremors induced by the excavation of a test facility at a depth of 420 m in granite. These authors defined the ratio R as

$$R = \frac{\mathrm{tr}(M_{ij}) \times 100}{|\mathrm{tr}(M_{ij})| + \sum |M_i^*|}. \tag{14}$$

FEIGNIER and YOUNG (1992) considered events to be tensile if $R > 30$, shear if $-30 \leq R \leq 30$, and implosive if $R < -30$.

Accordingly, values of R listed in Table 3 indicate that of the 10 events of this study, seven are clearly implosive and three are shear. The R values form two well-separated clusters, one in the range of 3 to 19 and the other extending from -56 to -66. Thus, this measure of the moment tensor confirms my previously stated observation that the source mechanisms tend to either have a substantial implosive component or none at all; these data do not indicate a continuum of implosive/deviatoric mixes. In contrast, the 33 R values listed in Table 1 of FEIGNIER and YOUNG (1992) show a fairly continuous distribution covering the range from -61 to 53.

Discussion

The results of analyzing the 10 events described here tend to confirm conclusions from earlier studies based on P-wave initial motions, to the effect that some mine-tremors appear to have double-couple mechanisms (e.g., SPOTTISWOODE, 1980; POTGIETER and ROERING, 1980) whereas others apparently have an implosive component (e.g., GANE, 1952; JOUGHIN, 1966; VAN DER HEEVER, 1982). More quantitatively, it has long since been realized that the energy release that causes mine tremors comes from the closure of the tabular excavations (stopes) as mining progresses (COOK, 1963). In fact, MCGARR (1976) related the seismic shear failure to the volume of stope closure according to

$$\sum M_0 = K\mu |\Delta V| \tag{15}$$

with $\frac{1}{2} \leq K \leq \frac{4}{3}$. The results listed in Table 2 for the seven events with negative moment tensor traces agree well with (15) but it is important to note that when I developed that equation I assumed that the time scale of volumetric closure was of the order of days and not coseismic. This admission notwithstanding, the important point is that the coseismic volume reduction estimated here (Table 2) agrees well with the expectations of how stope closure interacts with the rock mass to cause shear failure.

The shear/implosive mechanism indicated for seven of the events listed in Table 2 bears some resemblance to shear/implosive models proposed by TEISSEYRE (1980). RUDAJEV and SILENY (1985) and SILENY (1989) claimed confirmation of such models based on P- and S-wave amplitude distributions.

Perhaps the most fascinating and unexpected result is the finding that moment tensors fall into two, well separated, distinct categories in terms of the implosive/shear mix. It appears, so far, that tremors either have a coseismic closure volume of about 0.6 to 0.9 of the shear deformation, measured by $\sum AD$, or no closure volume. This effect is not understood.

Acknowledgements

This work was partly sponsored by the Air Force Technical Applications Center and the Air Force Geophysical Laboratory, Earth Sciences Division. I thank A. Rossouw, P. de Jong and S. M. Spottiswoode, of the Chamber of Mines of South Africa, and R. W. E. Green of the University of Witwatersrand for operating the GEOS station HBF on behalf of the USGS and for providing seismic data from the Klerksdorp seismic network. P. Mountfort and A. Van Zyl Brink kindly provided data from the Western Deep Levels network. J.Bicknell, E. Sembera, and R. Grose took part in the field experiments that yield ground motion data from the underground station HMN, W10 and W58. C. Mueller, L. Baker, and J. Langbein provided computer programs used here for analysis and presentation of results. This report benefited from insightful reviews by P. Spudich and J. Fletcher. C. Sullivan, C. Ramseyer and E. Dingel assisted considerably in the preparation of this manuscript.

REFERENCES

AKI, K., and RICHARDS, P., *Quantitative Seismology: Theory and Methods* (Freeman, Cooper, San Francisco, Calif. 1989).

BORCHERDT, R. D., FLETCHER, J. B., JENSEN, E. G., MAXWELL, G. L., VAN SCHAACK, J. R., WARRICK, R. E., CRANSWICK, E., JOHNSTON, M. J. S., and MCCLEARN, R. (1985), *A General Earthquake-observation System (GEOS)*, Bull. Seismol. Soc. Am. *75*, 1783–1825.

COOK, N. G. W., *The seismic location of rockbursts.* In *Proc. Fifth Rock Mechanics Symposium*, (Pergamon, New York 1963), pp. 493–516.

FEIGNIER, B., and YOUNG, R. P. (1992), *Moment Tensor Inversion of Induced Microseismic Events: Evidence of Nonshear Failures in the* $-4 < M < -2$ *Moment Magnitude Range*, Geophys. Res. Lett. *19*, 1503–1506.

GANE, P. G., SELIGMAN, P., and STEPHEN, J. H. (1952), *Focal Depths of Witwatersrand Tremors*, Bull. Seismol. Soc. Am. *42* 239–250.

GAY, N. C. (1975), *In situ Stress Measurements in Southern Africa*, Tectonophysics *29*, 447–459.

GAY, N. C., and WAINWRIGHT, E. H. eds. In *Proc. Ist Int. Conf. on Rockbursts and Seismicity in Mines* (SAIMM, Johannesburg 1984) 363 pp.

GAY, N. C., SPENCER, D., VAN WYK, J. J., and VAN DER HEEVER, P. K. (1984), *The control of geological and mining parameters in seismicity in the Klerksdorp mining district.* In *Proc. Ist Int. Conf. on Rockbursts and Seismicity in Mines* (SAIMM, Johannesburg 1984), pp. 107–120.

GELLER, R. J. (1976), *Body Force Equivalents for Stress Drop Seismic Sources*, Bull. Seismol. Soc. Am. *66*, 1801–1804.

GIBOWICZ, S. J., *The mechanism of seismic events induced by mining.* In *Proc. 2nd Int. Conf. on Rockbursts and Seismicity in Mines* (Balkema, Rotterdam 1990) pp. 3–27.

HANKS, T. C., and KANAMORI, H. (1979), *A Moment Magnitude Scale*, J. Geophys. Res. *84*, 2348–2350.

JOHNSON, L. R. (1974), *Green's Function for Lamb's Problem*, Geophys. J. *37*, 99–131.

JOST, M. L., and HERRMANN, R. B. (1989), *A Student's Guide to and Review of Moment Tensors*, Seismol. Res. Letters *60*, 37–57.

JOUGHIN, N. C. (1966), *The Measurement and Analysis of Earth Motion Resulting from Underground Rock Failure*, Ph.D. Thesis, Univ. of the Witwatersrand, Johannesburg, South Africa, 153 pp.

KNOPOFF, L., and RANDALL, M. J. (1970), *The Compensated linear-vector Dipole: A Possible Mechanism for Deep Earthquakes*, J. Geophys. Res. *75*, 4957–4963.

MCGARR, A. (1976), *Seismic Moments and Volume Changes*, J. Geophys. Res. *81*, 1487–1494.

MCGARR, A. (1991), *Observations Constraining Near-source Ground Motion Estimated from Locally Recorded Seismograms*, J. Geophys. Res. *96*, 16,495–16,508.

MCGARR, A. (1992), *An Implosive Component in the Seismic Moment Tensor of a Mining-induced Tremor*, Geophys. Res. Lett. *19*, 1579–1582.

MCGARR, A., and BICKNELL, J. (1990), *Synthetic seismogram analysis of locally recorded mine termors.* In *Proc. ISRM-SPE Int. Symp. Rock at Great Depth 3*, 1407–1413.

MCGARR, A., SPOTTISWOODE, S. M., and GAY, N. C. (1975), *Relationship of Mine Tremors to Induced Stresses and to Rock Properties in the Focal Region*, Bull. Seismol. Soc. Am. *65*, 981–994.

MCGARR, A., BICKNELL, J., SEMBERA, E., and GREEN, R. W. E. (1989), *Analysis of Exceptionally Large Tremors in Two Gold Mining Districts of South Africa*, Pure and Appl. Geophys. *129*, 295–307.

POTGIETER, G. J., and ROERING, C. (1984), *The influence of geology on the mechanisms of mining-associated seismicity in the Klerksdorp gold field.* In *Rockbursts and Seismicity in Mines* (eds. Gay, N. C., and Wainwright, E. C.) (SAIMM Symposium Series No. 6), (Johannesburg 1984) pp. 45–50.

RUDAJEV, V., and SILENY, J. (1985), *Seismic Events with Nonshear Components: II Rockbursts with Implosive Source Component*, Pure and Appl. Geophys. *123*, 17–25.

SILENY, J. (1989), *The Mechanism of Small Mining Tremors from Amplitude Inversion*, Pure and Appl. Geophys. *129*, 309–324.

SPOTTISWOODE, S. M. (1980), *Source Mechanism Studies on Witwatersrand Seismic Events*, Ph.D. Thesis, Univ. of Witwatersrand, Johannesburg, South Africa, 109 pp.

STICKNEY, M. C., and SPRENKE, K. F., *Seismic Events with Implosional Focal Mechanisms in the Coeur d'Alene Mining District, Northern Idaho*, J. Geophys. Res. in press.

STUMP, B. W., and JOHNSON, L. R. (1977), *The Determination of Source Properties by the Linear Inversion of Seismograms*, Bull. Seismol. Soc. Am. *67*, 1489–1502.

TEISSEYRE, R. (1980), *Some Remarks on the Source Mechanism of Rockbursts in Mines and on the Possible Source Extension*, Acta Montana *55*, 7–14.

VAN DER HEEVER, P. (1982), *The Influence of Geological Structure on Seismicity and Rockbursts in the Klerksdorp Goldfield*, M.S. Thesis, Rand Afrikans University, 160 pp.

VAN DER HEEVER, P. (1984), *Some technical and research aspects of the Klerksdorp seismic network.* In *Rockbursts and Seismicity in Mines* (eds. Gay, N. C., and Wainwright, E. H.) (SAIMM Symposium Series No. 6) (Johannesburg, South Africa) pp. 349–350.

WONG, I., and MCGARR, A., *Implosional failure in mining-induced seismicity: A critical review.* In *Rockbursts and Seismicity in Mines* (ed. Fairhurst, C.) (Balkema, Rotterdam 1990), pp. 45–51.

(Received October 6, 1992, accepted November 12, 1992)